International Journal of Mechanical and Production Engineering Research and Development (IJMPERD)
ISSN (P): 2249-6890; ISSN (E): 2249-8001
Vol. 8, Issue 2, Apr 2018, 1151-1160

USE OF BOND GRAPH TECHNIQUE FOR ROTOR DYNAMIC SYSTEM MODELLING AND COMPARATIVE ANALYSIS OF VIBRATION FREQUENCY USING FAST FOURIER TRANSFORM

ARKA SEN[1], MANIK CHANDRA MAJUMDER[2], NILOTPAL BANERJEE[3]
JAGANNATH DE[4], SUMIT MUKHOPADHYAY[5] & ROBIN KUMAR BISWAS[6]

[1, 2, 3, 4, 5] *Department of Mechanical Engineering, National Institute of Technology, Durgapur, India*

[6]*Department of Condition Monitoring and Structural Analysis, Central Mechanical Engineering Research Institute, Durgapur, India*

ABSTRACT

This paper presents the bond graph model of a vibrating ,rotating shaft with disc mounted on it. Unbalance mass fitted to the disc cause the disc to vibrate. The bond Graph technique has been used to model this vibrating system and SYMBOL Shakti software to simulate the model and determine the frequencies and their corresponding amplitudes.

KEYWORDS: Bond Graph, Rotor Dynamics, Vibration Analysis, Fast Fourier Transform, Amplitude Spectrum & Cross Power Spectrum

Received: Jul 27, 2017; **Accepted:** Aug 17, 2017; **Published:** Mar 23, 2018; **Paper Id.:** IJMPERDAPR2018133

Original Article

INTRODUCTION

Vibration in any machine is undesirable and can lead to catastrophic effects leading to the loss of manpower, machine and money and incurring a heavy loss to the operating cost of the plant. If the underlying causes are not corrected, the unwanted vibration itself can cause additional damage. There are several causes of vibration which may act alone or at random. Therefore, indicating such causes and bringing out their remedies is very essential in today's world. Keep in mind that vibration problems may be caused by auxiliary equipment, not just the primary equipment. These are some of the major causes of vibration. Vibration is a characteristic of virtually all industrial machines. On recording the vibration in the machine, if it appears to be above normal, then an insignificant wear will appear initially, but it's a prolonged which noise and heavy vibration then it calls for immediate maintenance action. Understanding why vibration occurs and how it manifests itself is a key first step toward preventing vibration from causing trouble in the production environment**.** Rotating machines elements like bearings, gears, fans, rotors, shafts are very common in every industry. Failure of these elements causes huge monitory losses. Condition monitoring of these elements can help in preventing the catastrophic failure of these elements, thereby saving downtime and monitory losses. The demand is increasing day by day for increasing the load carrying capacity, enhancing the performance and service life of mechanical systems. Failure of machines causes huge monitory losses. Fault diagnosis of mechanical systems can help in preventing the catastrophic failure, thereby saving downtime and monitory losses. Various condition monitoring techniques are available for fault diagnosis of mechanical systems e.g. acoustic emission, wear debris analysis, thermo-graph etc. Vibration monitoring is one of the most successful techniques used for condition monitoring of the mechanical

systems. Signal processing of vibration signals is very important for fault diagnosis of machines. Two independent parameters simultaneously direct the flow of energy in and out of any system and surroundings.

A bond graph is a domain -independent graphical description of the dynamic behavior of a physical system. The basic concept in the bond graph analysis is to specify the flow of energy in a system. In the bond graph method, these two parameters are defined by the general terms of Effort (e) and Flow (f).

The power of the instantaneous energy flow is the product of these two factors:

$$P(t) = e\,(t).f\,(t) \tag{1}$$

Momentum p and Displacement q are defined as:

$$p= \int e(t).dt \tag{2}$$

$$q=\int f(t).dt \tag{3}$$

Therefore, Energy (E) from equation Eq (1) is

$$E =\int e.f.\,dt = \int e(t).dq = \int f(t)\,dp$$

Using the principal of conservation of energy, the Bond graph model maps the flow of power through a system. By keeping track of the power in a system, the energy is accounted. Power is a convenient entity in modelling since it can be described as the multiplication of two conjugate variables regardless of the engineering domain of its origin. A bond graph maps the power flow through a system and simultaneously describes the relationships between the conjugate variables in each branch of the system. In this way, an accounting of all the energy of a system, and the conjugate variable relationships are used to develop the describing equations of a system.

MATERIALS AND METHODOLOGY

Experimental Setup and Procedure of Data Collection

An experimental set up was built based on model based on the model-based technique for identification of vibration. The experimental verification of the Unbalance Identification of mass on a shaft with a single plane and two eccentricity locations has been performed on a Machine Fault Simulator Test Rig which was available at CMERI Durgapur.

A rigid shaft considered to be massless is mounted between two roller bearings. The distance between the two bearings is L1+L2, which is 60cm. The rotor shaft and the VFD Drive motor are connected through a flexible coupling. To measure the vibration in X-Direction and Y-Direction at the two bearings, four accelerometers are connected; two in each bearing. The weight of the disc is 653 gram (M1). The disc position id varied with respect to three positions as shown in Figure 6, 7 and 8 respectively. Three unbalance masses of 8 gram (m1), 12 gram (m2) and 16 gram (m3) are attached, subsequently to the disc at eccentricities 6.85cm (e1) and 6.85cm (e2) separately one by one. Then the shaft is rotated at rpm 300, 600, 900, 1200 and 1500; and simultaneously the vibration readings (RMS values) and their phase values in x and y-direction at the two bearings were noted down. Artificial Neural Networking Techniques with varying training algorithms have been used to determine the unbalance plane of vibration.

Mass Unbalance: The unbalance masses used are 8 grams, 12 grams and 16 grams, which are shown in the figures below.

Figure 1

Figure 2

Figure 3

Figure 1: Unbalance mass of 8gram attached to the rotating system; Figure 2: Unbalance mass of 10gram attached to the rotating system; Figure 3: Unbalance mass of 8gram attached to the rotating system

Eccentricity

All rotors have some eccentricity. Eccentricity is present when the geometrical center of the rotor and the mass center do not coincide along their length. In the present case, the disc is considered absolutely balanced where the Geometrical Center of the disc coincides with the Centre of the Gravity of the disc. In the current research work eccentricity is the distance between the Geometrical Centre (Centre of rotation) and the points where the unbalance mass is to be attached. There are two locations at a distance of 6.85cm from the center of rotation (e1) and at a distance of 4.85cm from the center of rotation of the disc (e2).

Figure 4: The Rotating Disc

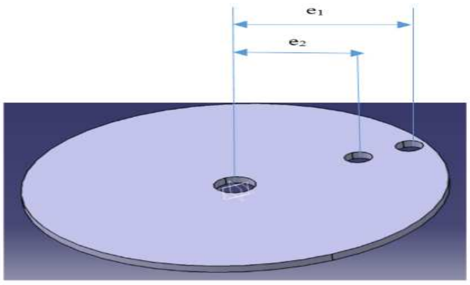

Figure 5: Schematic Representation of Rotating Disc

Plane of Unbalance

The Figure 6, Figure 7 and Figure 8 shows the different position of the rotating disc placed on the shaft (left, center and right respectively).

Figure 6

Figure 7

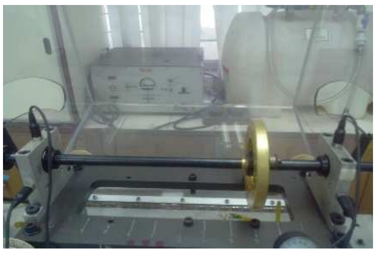

Figure8

The design of experiments (Table 2) is based on the maximum possible combination of Unbalance mass (m), Eccentricity (e), Plane of unbalance (p) and the RPM (r) values. The table (Table 1) below provides the maximum and minimum values the independent parameters/input to the system.

Table 1: Independent/Input Parameters and Their Levels

Serial No	Independent /Input Parameters	Minimum Level	Maximum Level
1	Unbalance Mass (m)	8gram	16gram
2	Eccentricity (e)	4.85cm	6.85cm
3	Plane of unbalance (p)	15cm (measured from left bearing)	45cm (measured from left bearing)
4	Revolutions per Minute (RPM) (r)	300	1500

Table 2: Design of Experiment

Set	Experimental Codes	Unbalance Mass	Eccentricity	Location of Unbalance Plane (in cm)
		(in Gram)	(in cm)	*(From Left Bearing)*
1	NFL	0	0	15
2	NFC	0	0	30
3	NFR	0	0	45
4	L8e2	8	4.85	15
5	C8e2	8	4.85	30
6	R8e2	8	4.85	45
7	L8e1	8	6.85	15
8	C8e1	8	6.85	30
9	R8e1	8	6.85	45
10	L12e2	12	4.85	15
11	C12e2	12	4.85	30
12	R12e2	12	4.85	45
13	L12e1	12	6.85	15
14	C12e1	12	6.85	30
15	R12e1	12	6.85	45
16	L16e2	16	4.85	15
17	C16e2	16	4.85	30
18	R16e2	16	4.85	45
19	L16e1	16	6.85	15
20	C16e1	16	6.85	30
21	R16e1	16	6.85	45

The design of experiments as mentioned in the table 2 has been performed for 300, 600, 900, 1200 and 1500 RPM`s. In total there are 105 sets of experiments.

INDICATORS USED IN EXPERIMENT

NFC: No fault disc at Centre, **NFL**: No fault disc at a Left position, **NFR**: No fault disc at a Right position.

The number succeeding NFC, NFL, and NFR represents the rpm at which the disc is rotating without any unbalance mass attached. With unbalance mass attached, the experimental code is written in the following format as mentioned below one after the other.

Position of Rotating Disc (p) Unbalance Mass (m) Eccentricity (e) Revolutions Per Minute (RPM) (r)

For example:C16e11500 represents the rotating disc placed at center of the shaft with mass unbalance of 16gram placed at an eccentricity e1rotated at 1500 RPM. It is similarto the rest of the experimental cases.

Bond Graph Model for the Rotating System with Unbalance Mass

A bond graph model has been created for the rotating shaft – disc system supported on two bearings which are

shown below.

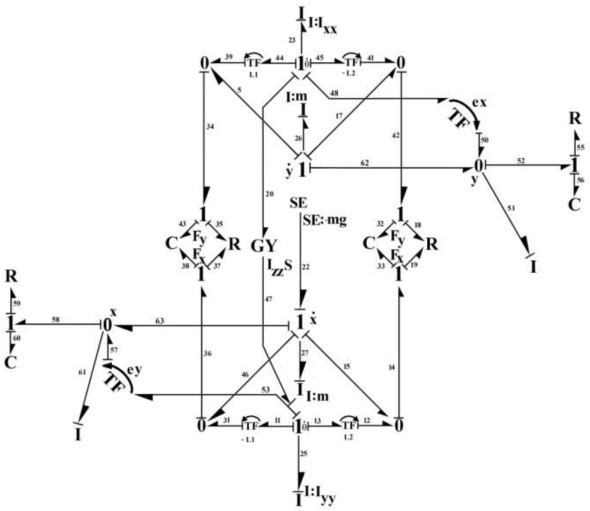

Figure 9: Bond Graph Model of the Rotating System

The center of mass of the system is modelled by four 1-junctions along the center line of the figure. Two of them model the angular velocity and two of them model the translational velocity with proper subscripts x and y respectively. 1$\dot{\theta}$xjunction and 1$\dot{\theta}$y junction represents the angular velocity of the center of mass of the system about X and Y axes respectively. Similarly,1$\dot{x}$ and 1$\dot{y}$represent its translational velocity in X and Y axes respectively. A two-port element G_Y with modulus I_{zz} times spin of the rotor models the gyroscopic coupling between the two one junctions representing the angular velocity about X and Y axes. C - R field on the left hand side and the right-hand side represent the two bearings on which the rotor is supported, where the stiffness and damping are given by C element and R element of the field. The resultant linear motion due to angular and translational velocity associated with a Y-direction is summed up in the 0-junction appended to bond 39 and 34. T_F element linked with bond number 44 and 39 converts the angular motion about X—axis into linear motion in Y- direction corresponding to a mass center of the bearing (LHS), the transformer modulus being equal to the linear distance between the disc and the bearing center (L_1). Similarly, motion of the center of mass of the bearing associated with Y direction is also modeled. Same is the case for the right -hand side (RHS) bearing also.

Unbalance Mass at a distance e (eccentricity) from the center of the disc is modeled as a lumped mass point on the disc. The motion in rotating y -direction is obtained by summing up the linear motion from 1$\dot{y}$ and converting the angular motion from 1$\dot{\theta}$x by multiplying with Transformer modulus e_X at 0y junction. Similarly, the motion in rotating x -direction is obtained by summing up the linear motion from 1$\dot{x}$ and converting the angular motion from 1$\dot{\theta}$y by multiplying with Transformer modulus ey at 0x junction. Instantaneous values of e_x and e_y are equal to e times cosωtand e times sinωt respectively. With these 0x and 0y junctions I elements represent the unbalance mass. However, to avoid differential causality, C and R elements appended through 1-junctions on both sides to model hypothetical contact flexibility between the lumped unbalance mass and the disc.

Source of Effort (SE element) is connected to the 1$\dot{x}$ junction with a value of –mg to designate the weight of the rotor system. The negative sign shows that the weight acts in the negative x-direction.

RESULTS AND DISCUSSIONS

In this current paper, a particular case of 16 gram unbalance placed on the disc at eccentricity e1 is being considered. The disc is placed at the center of the shaft which is rotated at 1500RPM using a variable frequency drive motor. For unbalance faults, frequency peaks are shown at 1X RPM. In any rotating system, misalignment and bearing faults are evident, hence the Peaks at 2X and higher frequencies are reflected in the Amplitude spectrum. In the current case frequency peak at 25HZ

Experimental Setup C16E11500 denotes that the Disc is placed at Centre with 16-gram unbalance mass placed at eccentricity e1and rotated at 1500 rpm.

The cross Power spectrum of the particular signal as shown in figure 11, 13, 15, and 17 determines the power shared by a given frequency of the two signals using its squared module, and the phase shift between the two signals at that frequency using its argument. It is generally used for non-finite energy signals (mostly not limited in time signals), who aren't square-summable. The signal's PSD is the autocorrelation of the signal's Fourier Transform, as stated by the Wiener–Khinchin theorem.

Left Bearing X-Direction (Channel-2)

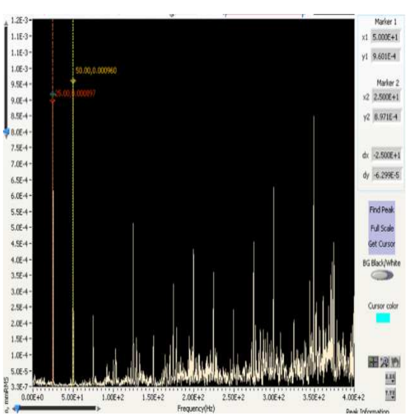

Figure 10: Channel-2 Amplitude Spectrum

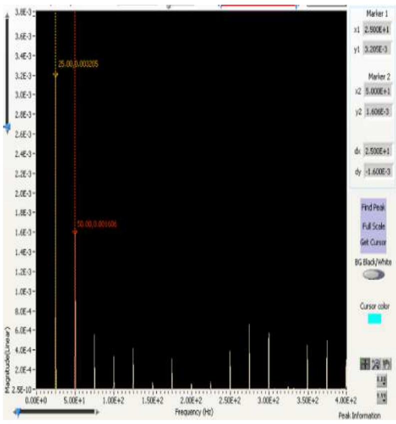

Figure 11: Channel-2 – Cross Power Spectrum

Left Bearing Y- Direction (Channel-7)

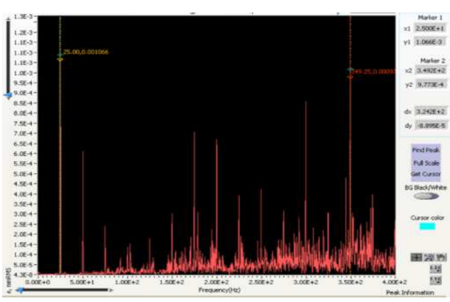

Figure 12: Channel-3 – Amplitude Spectrum

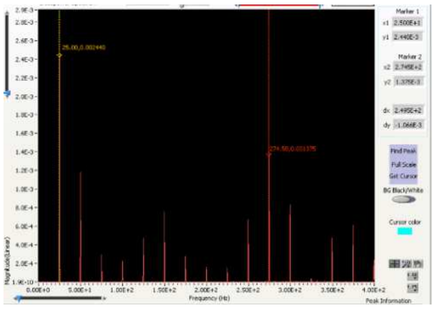

Figure 13: Channel-3 – Cross Power Spectrum

Right Bearing X- Direction (Channel-3)

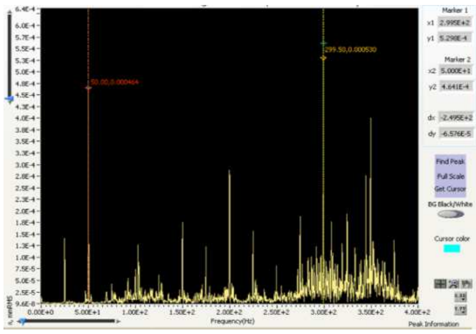

Figure 14: Channel 7- Amplitude Spectrum

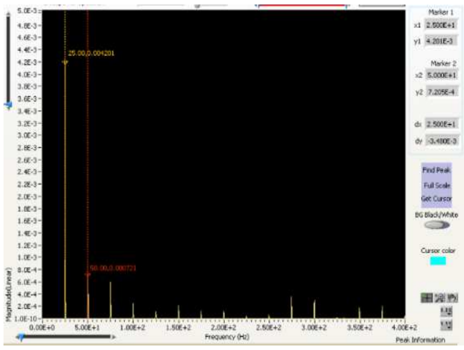

Figure 15: Channel 7 – Cross Power Spectrum

Right Bearing Y-Direction (Channel-8)

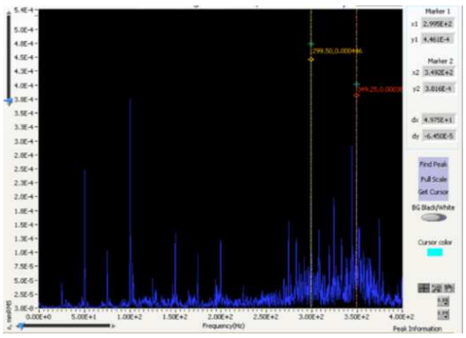

Figure 16: Channel 8 - Amplitude Spectrum

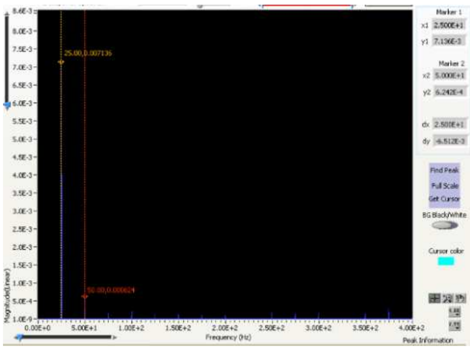

Figure 17: Channel 8 - Cross Power Spectrum

Bond Graph Results after Simulation

The bond graph model representing the rotating shaft on two roller bearings is shown in Figure 9. The simulated FFT results from bond graph analysis depicting frequency peaks at 25Hz is shown in Figure 18-21. From the figure, it is clearly evident that the vibration in Y-direction is much more than that of the X-direction.

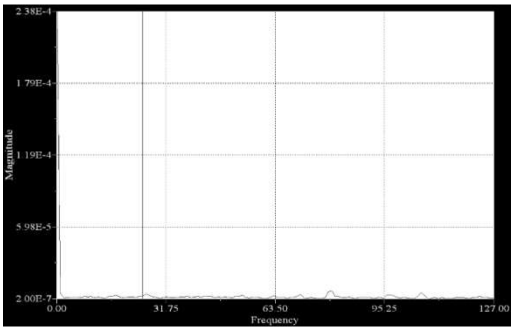

Figure 18: FFT for Left Bearing X-Direction

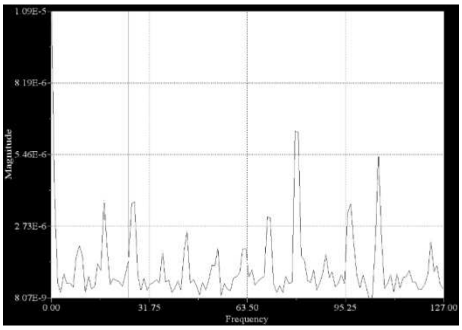

Figure 19: FFT for Left Bearing Y-Direction

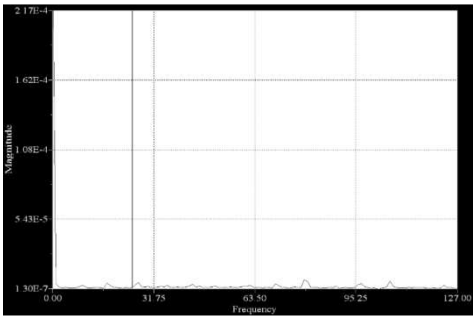

Figure 20: FFT for Right Bearing X-Direction

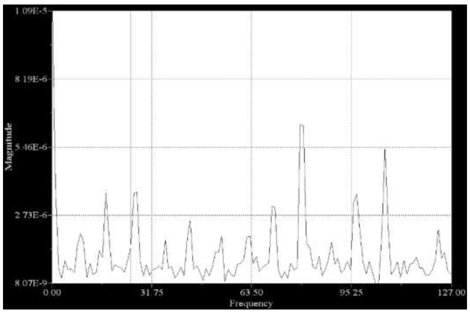

Figure 21: FFT for Right Bearing Y-Direction

The values of amplitude spectrum (from experiment), cross power spectrum and amplitude values from the bond graph simulation has been tabularized in the Table 3.

Table 3: Comparative Analysis of Data

Bearing Location	Frequency (1X RPM) for Unbalance	Amplitude Spectrum (mm RMS)	Cross Power Spectrum (Magnitude Linear)	FFT Analysis (Bond Graph) [Amplitude (mm)]
Left Bearing X-Direction (Channel-2)	25 Hz	.001201	.003205	.002305
Left Bearing Y-Direction (Channel-3)	25Hz	.001101	.002440	.001437
Right Bearing X-Direction (Channel-7)_	25Hz	.001459	.004201	.001241
Right Bearing Y-Direction (Channel-8)	25Hz	.002478	.007136	.001434

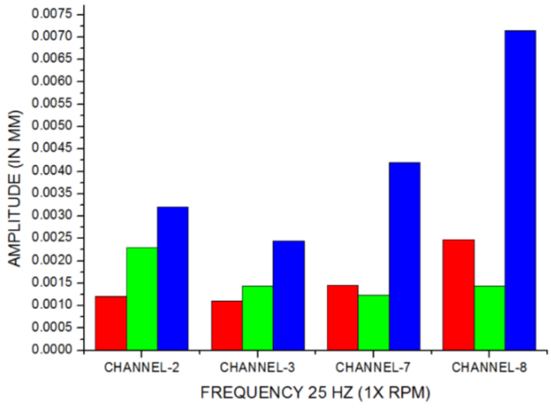

Figure 22: Bar Chart Showing Comparative FFT Analysis

- Amplitude Spectrum (mm RMS) [Experimental]
- FFT Analysis (Bond Graph) [Amplitude (mm)]
- Cross Power Spectrum (Magnitude Linear)

The bar chart showing comparative FFT analysis between the amplitude of vibrations at a 1X RPM, frequency and the bond graph simulated output. The difference between the experimental values and the simulated values is significantly less (in some cases it is as less as.001mm) which is clearly shown in Figure 15. This validates the Bond Graph model for the proposed rotor dynamic system.

CONCLUSION AND FUTURE SCOPE OF WORKS

In this paper, a new approach has been discussed with respect to the modeling of a rotating system with unbalance fault. The Bond Graph approach is very convenient and can be used for any dynamic system analysis. Using Fast Frequency Transform in Bond Graph simulation, frequency peaks and their amplitude have been determined and compared with the experimental results. The same technique can further be extended for other faults detection and identification in a rotating system.

ACKNOWLEDGEMENTS

The author is thankful to the Department of Mechanical Engineering, National Institute of Technology ,Durgapur and Condition Monitoring and Structural Analysis, Department of Central Mechanical Engineering Research Institute located at Durgapur to help me to carry out this research work on “Modelling of a Rotor Dynamic System using Bond Graph Technique and Comparative Analysis of Vibration Frequency using Fast Fourier Transform”.

REFERENCES

1. *R. J. Kuo, Intelligent Diagnosis for Turbine Blade Faults Using Artificial Neural Networks and Fuzzy Logic, Engineering Application Artificial Intelligence. Vol. 8, No. 1, pp. 25-34, 1995.*
2. *Yuan-Pin Shih and An-Chen Lee, Identification of the unbalance distribution in flexible rotors, Int. J. Mech. Sci. Vol. 39, No. 7, pp. 841 857, 1997.*
3. *K N Gupta, Vibration - A tool for machine diagnostics and condition monitoring, Sadhana, Vol. 22, Part 3, June 1997, pp. 393-410.*
4. *Jae Hong Suh, Soundar R. T. Kumara (I), Shreesh P. Mysore, Machinery Fault Diagnosis and Prognosis: Application of Advanced Signal Processing Techniques, Annals of the ClRP Vol. 48/7/7999 317.*
5. *Roya Javadpour, Gerald M. Knapp, A fuzzy neural network approach to machine condition monitoring, Computers & Industrial Engineering 45 (2003) 323–330.*
6. *Jason R. Blough, A survey of DSP methods for rotating machinery analysis what is needed, what is available, Journal of Sound and Vibration 262 (2003) 707–720.*
7. *Ashwani Sharma & M. A. Murtaza , Modeling and Finite Element Analysis of Vertical Axis Wind Turbine Rotor Configurations, International Journal of Mechanical and Production Engineering Research and Development (IJMPERD), Volume 6, Issue 3, May- June 2016, pp. 23-34*
8. *Peter W. Tse, Wen-Xian Yang, H. Y. Tam, Machine fault diagnosis through an effective exact wavelet analysis, Journal of Sound and Vibration 277 (2004) 1005–1024.*
9. *D. F. Shi, F. Tsung, P. J. Unsworth, Adaptive time–frequency decomposition for transient vibration monitoring of rotating machinery, Mechanical Systems and Signal Processing 18 (2004) 127–141.*

10. *Z. K. Peng, F. L. Chu, Application of the wavelet transform in machine condition monitoring and fault diagnostics: a review with bibliography, Mechanical Systems and Signal Processing 18 (2004) 199–221.*
11. *YazhaoQiu, Singiresu S. Rao, A fuzzy approach for the analysis of unbalanced nonlinear rotor systems, Journal of Sound and Vibration 284 (2005) 299–323*
12. *Bo-Suk Yang, Dong-Soo Lib, Andy Chit Chiow Tan, VIBEX: an expert system for vibration fault diagnosis of rotating machinery using decision tree and decision table, Expert Systems with Applications 28 (2005) 735–742*
13. *B Liu, Selection of wavelet packet basis for rotating machinery fault diagnosis, Journal of Sound and Vibration 284 (2005) 567–582.*
14. *Michael Feldman, Time-varying vibration decomposition and analysis based on the Hilbert transform, Journal of Sound and Vibration 295 (2006) 518–530*
15. *Jiangping Wang, Hongtao Hu, Vibration-based fault diagnosis of pump using fuzzy technique, Measurement 39 (2006) 176–185.*
16. *Andrew K. S. Jardine, Daming Lin, Dragan Banjevic, A review on machinery diagnostics and prognostics implementing condition-based maintenance, Mechanical Systems and Signal Processing 20 (2006) 1483–1510.*